New Phytologist

Research

Priority report

The GABA shunt contributes to ROS homeostasis in guard cells of Arabidopsis

Authors for correspondence:
Bo Xu
Email: b.xu@adelaide.edu.au

Matthew Gilliham
Email: matthew.gilliham@adelaide.edu.au

Received: *15 August 2023*
Accepted: *23 October 2023*

Bo Xu[1]*, Xueying Feng[1]*, Adriane Piechatzek[1], Shuqun Zhang[2], Kai R. Konrad[3], Johannes Kromdijk[4], Rainer Hedrich[3] and Matthew Gilliham[1]

[1]Plant Transport and Signalling Lab, ARC Centre of Excellence in Plant Energy Biology, School of Agriculture, Food and Wine & Waite Research Institute, Glen Osmond, SA, 5064, Australia; [2]Division of Biochemistry, University of Missouri, Columbia, MO 65211, USA; [3]Institute for Molecular Plant Physiology and Biophysics, University of Wuerzburg, Julius von-Sachs Platz 2, D-97082, Würzburg, Germany; [4]Department of Plant Sciences, University of Cambridge, Downing St., Cambridge, CB2 3EA, UK

New Phytologist (2023)
doi: 10.1111/nph.19390

Key words: calcium, EGTA, *gad2-1*, *gad2-2*, H_2DCF-DA, stomatal apertures.

Summary

- γ-Aminobutyric acid (GABA) accumulates rapidly under stress via the GABA shunt pathway, which has been implicated in reducing the accumulation of stress-induced reactive oxygen species (ROS) in plants.
- γ-Aminobutyric acid has been demonstrated to act as a guard-cell signal in *Arabidopsis thaliana*, modulating stomatal opening. Knockout of the major GABA synthesis enzyme *Glutamate Decarboxylase 2* (*GAD2*) increases the aperture of *gad2* mutants, which results in greater stomatal conductance and reduces water-use efficiency compared with wild-type plants.
- Here, we found that the additional loss of *GAD1*, *GAD4*, and *GAD5* in *gad2* leaves increased GABA deficiency but abolished the more open stomatal pore phenotype of *gad2*, which we link to increased cytosolic calcium (Ca^{2+}) and ROS accumulation in *gad1/2/4/5* guard cells. Compared with wild-type and *gad2* plants, glutamate was ineffective in closing *gad1/2/4/5* stomatal pores, whereas lowering apoplastic calcium, applying ROS inhibitors or complementation with *GAD2* reduced *gad1/2/4/5* guard-cell ROS, restored the *gad2*-like greater stomatal apertures of *gad1/2/4/5* beyond that of wild-type.
- We conclude that GADs are important contributors to ROS homeostasis in guard cells likely via a Ca^{2+}-mediated pathway. As such, this study reveals greater complexity in GABA's role as a guard-cell signal and the interactions it has with other established signals.

Introduction

γ-Aminobutyric acid (GABA) is a nonproteinogenic amino acid predominantly synthesized from glutamate (Glu) by glutamate decarboxylase (GAD) in the cytosol. γ-Aminobutyric acid synthesis constitutes the first step of a three-step pathway known as the GABA shunt that provides an alternative route for the production of succinate from α-ketoglutarate via the mitochondrial-based tricarboxylic acid (TCA) cycle (Bouché *et al.*, 2003). Critically, the GABA shunt bypasses two reactive oxygen species (ROS)-inhibited reactions of the TCA cycle during stress events (Bouché *et al.*, 2003; Bown & Shelp, 2016). The GABA shunt has been traditionally proposed to have a role in pH regulation, carbon–nitrogen balance, and modulating ROS under stress, although the mechanics of how GABA confers its influence on these processes is not well-understood (Ramesh *et al.*, 2017; Fromm, 2020; Xu *et al.*, 2021b).

In *Arabidopsis thaliana*, there are five *GAD* isoforms (*GAD1–5*), all with distinct expression patterns (Scholz *et al.*, 2015). *GAD1* and *GAD2* are the most highly expressed, predominantly in the roots and shoots, respectively (Scholz *et al.*, 2015). GAD1 controls GABA accumulation in roots particularly under heat stress (Bouché *et al.*, 2004), whilst GAD2 catalyses GABA synthesis in leaves (Xu *et al.*, 2021a). The other three *GAD* genes normally have very low,

*These authors contributed equally to this work.

barely detectable, transcription (Scholz *et al.*, 2015), but are stimulated to catalyse GABA production under certain stresses, such as bacterial infection (Deng *et al.*, 2020) or combined high light and heat (Balfagón *et al.*, 2022). γ-Aminobutyric acid deficiency in leaves following the simultaneous loss of *GAD1* and *GAD2* was observed to result in higher stomatal conductance in *gad1/2* plants (Mekonnen *et al.*, 2016). Xu *et al.* (2021a) found that the loss of just *GAD2* led to more open stomatal pores and greater transpiration rates, and that wild-type-like stomatal phenotypes in *gad2* leaves could be restored by guard-cell-specific complementation with *GAD2*. *GAD* mutants have also been shown to be more susceptible to stress, for instance, *gad1/2* double mutants exhibited enhanced salt- and hypoxia-sensitivity (Mekonnen, 2017; Su *et al.*, 2019; Wu *et al.*, 2021), and whilst *gad2* mutants are less drought-tolerant than wild-type (WT) plants, *GAD2* overexpression in a WT background improved drought tolerance (Xu *et al.*, 2021a,b). Alongside other evidence this added significant weight to the proposal that, in guard cells at least, GABA has a signalling role (Bouché *et al.*, 2003; Ramesh *et al.*, 2015; Bown & Shelp, 2016; Fromm, 2020; Xu *et al.*, 2021a,b).

After GABA synthesis by GAD, cytosolic GABA is shuttled into the mitochondria and degraded by GABA transaminase (GABA-T) into succinic semialdehyde (SSA), and into succinate by succinic semialdehyde dehydrogenase (SSADH). The *A. thaliana* genome has a single *GABA-T* gene; its knockout in the *gaba-t* mutant (a.k.a. *pop2*) completely disrupts GABA degradation via the GABA shunt and results in GABA overaccumulation, impairing pollen tube growth and reducing plant fertility (Palanivelu *et al.*, 2003). *gaba-t*/*pop2* plants do not have any obvious vegetative growth defects, but the resulting GABA overaccumulation improves salt and hypoxia tolerance, which has been linked to ROS reduction (Su *et al.*, 2019; Wu *et al.*, 2021). Knockout of the last step of the GABA shunt, SSADH, results in increased ROS production, necrotic lesions, and dwarfism (Fait *et al.*, 2005). Exogenous GABA treatment has also been proposed to reduce ROS via upregulation of antioxidant enzymes through an unknown mechanism (Shi *et al.*, 2010).

Here, we use the quadruple *gad1/2/4/5* mutant to further examine the role of the GABA shunt in ROS homeostasis. We find that the *gad1/2/4/5* mutant, which maintains very low GABA accumulation (Deng *et al.*, 2020), is found to reverse the large stomatal pore phenotype seen in *gad2* plants due to significantly greater ROS accumulation in its guard cells. To further summarize, despite their minor role in GABA accumulation in leaves, ablation of either *GAD4* and/or *GAD5* in addition to *GAD1* and *GAD2* was sufficient to result in the elevation of guard-cell ROS production and was associated with a higher resting cytosolic Ca^{2+} in the guard cells of *gad1/2/4/5*. The addition of ROS inhibitors, apoplastic calcium chelation, or introducing an active *GAD2* (via *GAD2Δ*) reduced ROS accumulation in *gad1/2/4/5* guard cells and revealed the clear negative relationship between GABA accumulation and stomatal conductance that exists when ROS is low. Our data show the importance of the GABA shunt in regulating ROS production in guard cells and introduces new interaction points for GABA as a plant signalling molecule.

Materials and Methods

Plant materials and growth conditions

All experiments were performed on *Arabidopsis thaliana* (L. Heynh) WT and mutant plants in the Col-0 background, grown in soil containing coco peat/Irish peat (1 : 1 ratio) under short day conditions (100–120 μmol m^{-2} s^{-1}, 10 h : 14 h, light : dark) at 22°C and 50–60% relative humidity for 5–6 wk. The T-DNA insertional mutants, *gad1* (SALK_017931), *gad2-1* (GABI_474_E05), and *gad2-2* (SALK_028819), were obtained from the Arabidopsis Biological Resource Centre (ABRC). The *gad1/2/4/5* mutant was made for Deng *et al.* (2020). The *gad1/2*, *gad1/2/4*, and *gad1/2/5* mutants were segregated following the cross of *gad2-1* × *gad1/2/4/5* and selected using PCR with primers described in Supporting Information Table S1. The vector of pCAMBIA3300 carrying a Ca^{2+} (R-GECO1) and pH (PRpHluorin) dual sensor (CapHensor) (Li *et al.*, 2021) and the vector containing *GAD2Δ* driven by a guard cell promoter (*GC1*) (Xu *et al.*, 2021a) were stably expressed in Arabidopsis WT and mutant plants via *Agrobacterium tumefaciens* floral dip-mediated transformation.

Stomatal aperture and density measurements

All chemicals were obtained from Sigma-Aldrich. Epidermal strips were peeled from abaxial sides of leaves (Xu *et al.*, 2021a), pre-incubated in stomatal measurement buffer containing 10 mM KCl, 5 mM L-malic acid, 10 mM 2-ethanesulfonic acid (MES), adjusted to pH 6.0 with 2-amino-2-(hydroxymethyl)-1,3-propanediol (Tris) under light (200 μmol m^{-2} s^{-1}) for 1 h, then were transferred to the same buffer +/− supplementation with 50 μM $CaCl_2$, 1 mM GABA, 1 mM glutamate, 5 mM $LaCl_3$, 200 μM (or 1 mM) ethylene glycol tetraacetic acid (EGTA), 20 μM diphenyleneiodonium chloride (DPI), 2 mM salicylhydroxamic acid (SHAM), and/or 100 U ml^{-1} catalase as indicated in figure legends, and incubated under light for another 2 h before measurement. Stomata on epidermal peels were imaged using an Axiophot Pol Photomicroscope (Carl Zeiss), and stomatal aperture was analysed using ImageJ (http://rsbweb.nih.gov/ij/; Schneider *et al.*, 2012). All stomatal aperture measurement were taken as blind treatments and repeated at least twice from different batches of plants and the whole experimental procedure was performed between 2 h after lights on and 3 h before lights off. The stomatal conductance was determined using the AP4 Porometer (Delta-T Devices, Cambridge, UK) and calculated based on the mean value from 2 to 3 leaf recordings per plant, as described in Xu *et al.* (2021a). For Arabidopsis stomatal density measurement, epidermal strips were peeled from abaxial sides of mature leaves, three leaves per plants using three plants for each genotype and imaged using an Axiophot Pol Photomicroscope (Carl Zeiss).

Quantification of ROS and NO production in guard cells

Reactive oxygen species and NO measurement in guard cells followed modified methods previously described by Zhu *et al.* (2016) and Agurla *et al.* (2016), respectively. Briefly, epidermal

strips were peeled from the abaxial sides of leaves, following the same treatment and process as for the stomatal aperture assay, before ROS staining in a stomatal measurement buffer containing 30 μM 2′,7′-dichlorofluorescin diacetate (H_2DCF-DA) for 20 min, or NO staining in the stomatal measurement buffer containing 20 μM 4,5-diaminofluorescein diacetate (DAF-2DA) for 30 min in dark. The fluorescence of H_2DCF-DA or DAF-2DA dye in guard cells of epidermal strips was captured using a Nikon A1R laser scanning confocal microscope with a laser power of 1% (excitation = 488 nm and emission = 525–575 nm). The mean ROS and NO fluorescence intensity of guard cell pair regions of interest (ROI) was analysed by ImageJ (http://rsbweb.nih.gov/ij/; Schneider *et al.*, 2012), following image processing guidelines as described in Zhu *et al.* (2016) and Agurla *et al.* (2016).

GABA and glutamate quantification

Rosette leaves were excised, snap-frozen in liquid nitrogen, and homogenized in liquid nitrogen. Approximately 50 mg fresh tissue was used to analyse GABA and Glu content using the Acquity Ultra Performance Liquid Chromatography (UPLC) System (Waters) with a Cortecs or Phenomenex UPLC C18 column (1.6 μm, 2.1 × 100 mm) as described previously in Xu *et al.* (2021a), or using 100 mg fresh tissue for GABA quantification with the GABase enzyme assay, as described previously in Ramesh *et al.* (2018).

Guard-cell Ca^{2+} and pH imaging

Approximately 5-wk-old Arabidopsis seedlings stably expressing the CapHensor driven by a 35S promoter (Li *et al.*, 2021) were used to determine the relative cytosolic Ca^{2+} ($[Ca^{2+}]_{cyt}$) and H^+ ($[H^+]_{cyt}$) concentration ratio in guard cells. Leaf 8 was detached, placed on MilliQ water-soaked 3MM Whatman filter paper, and covered in a Petri dish for 10 min to rest cytosolic Ca^{2+} and pH at room temperature. Then, the leaf abaxial surface was placed and adhered to a glass-bottom culture dish (Ø35 mm petri dish, Ø14 mm microwell; MatTek, Ashland, MA, USA) using silicone-based medical adhesive (NFS Adhesive B-531, Factor II), and topped with 2 ml of stomatal buffer (5 mM KCl, 2.5 mM L-malic acid and 5 mM MES/Tris, pH 6.0) before imaging. For pH and Ca^{2+} imaging, the fluorescence of PRpHluorin was excited sequentially at 400 nm, 415 nm (isosbestic point), and 470 nm using a High-Power LED Collimator Source (Mightex, Pleasanton, CA, USA) and captured by an inverted Nikon Ti E Live Cell Microscope (Nikon, Rhodes, NSW, Australia) with a 515–555 nm filter, followed by the fluorescence of R-GECO1 excited at 540 nm and captured with a 590–650 nm filter by the same light source and microscope. Fluorescence intensity of PRpHluorin and R-GECO1 from guard cells was analysed by NIS-Elements Advanced Research (Nikon) and further used to calculate relative H^+ ratio and Ca^{2+} ratio as described in Li *et al.* (2021) using the equations:

$$[H^+]_{cyt} \text{ ratio } 470 \text{ nm}/400 \text{ nm} = \frac{\text{PRpHlurion fluorescence at } 470 \text{ nm}}{\text{PRpHlurion fluorescence at } 400 \text{ nm}}$$

$$[Ca^{2+}]_{cyt} \text{ ratio } 540 \text{ nm}/415 \text{ nm} = \frac{\text{R-GECO1 fluorescence at } 540 \text{ nm}}{\text{PRpHlurion fluorescence at } 415 \text{ nm}}$$

Results and Discussion

Glutamate Decarboxylase 2 is the major *GAD* isoform expressed in leaves and its ablation results in greatly reduced leaf GABA accumulation, more open stomata than for WT seedlings, greater stomatal conductance, and drought susceptibility (Xu *et al.*, 2021a). Here, we observe that the loss of *GAD1*, *GAD4*, and *GAD5* in *gad2-1* plants further reduced GABA content in the leaves of the quadruple *gad1/2/4/5* mutant (Fig. 1a; Deng *et al.*, 2020). Surprisingly, *gad1/2/4/5* had WT-like stomatal conductance and stomatal aperture, and not the greater conductance and aperture of *gad2* (Fig. 1b,c; Xu *et al.*, 2021a); all three genotypes had the same stomatal density (Fig. 1d), indicating the differences in stomatal conductance were likely due to differences in stomatal apertures.

Both *gad2-1* and *gad1/2/4/5* possess the same T-DNA insertion within the *GAD2* (At1g65960) gene, derived from the GABI-Kat (GABI_474_E05) seed collection (Deng *et al.*, 2020; Xu *et al.*, 2021a). To investigate the individual impact of additional *gad* mutations, we crossed *gad2-1* with *gad1/2/4/5*. The first generation F_1 *gad2-1* × *gad1/2/4/5* progeny exhibited greater stomatal conductance than *gad1/2/4/5* and WT plants, similar to *gad2-1* plants, as could be expected as it is homozygous for *gad2-1* but heterozygous for all other *gad* mutations (Fig. 2a). We continued segregation of F_1 plants to produce double and triple *gad* knockout mutants to determine whether we could identify the *gad* mutations that compromised the *gad2-1* phenotype. Consistent with the previous research (Mekonnen *et al.*, 2016; Xu *et al.*, 2021a), the *gad1/2* double mutant had similarly high stomatal conductance and aperture to *gad2-1*, whilst *gad1*, *gad1/2/4*, and *gad1/2/5* had WT-like stomatal phenotypes (Figs 2b, S1a). Note that *gad1* was the mother line of the original *gad1/2/4/5* mutant and was analysed alongside our cross, not derived from it. Furthermore, we suspect that the variation in stomatal conductance for *gad1/2* (unlike previously detected; Mekonnen *et al.*, 2016) was due to this genotype being measured over a series of days due to the scale of the experiment. All the generated *gad* mutants significantly reduced GABA accumulation in leaf tissue, unlike *gad1* (Fig. S1b). Consistent with *GAD1* being predominantly expressed in the roots and previous reports of its mutation affecting GABA accumulation mainly in roots (Bouché *et al.*, 2004; Scholz *et al.*, 2015; Mekonnen *et al.*, 2016), *gad1* mutants did not have altered stomatal apertures. Collectively, these data suggest that the loss of *GAD4* and/or *GAD5* in addition to *GAD2* is the likely foundational cause for abolishing the *gad2* stomatal phenotype of *gad1/2/4/5* plants.

Glutamate Decarboxylase synthesizes GABA from glutamate (Glu), which, in addition to its role as a carbon–nitrogen cycle intermediate and proteinogenic amino acid (unlike GABA) is proposed to act on glutamate receptor-like (GLR) proteins to trigger calcium signalling and activate downstream responses such

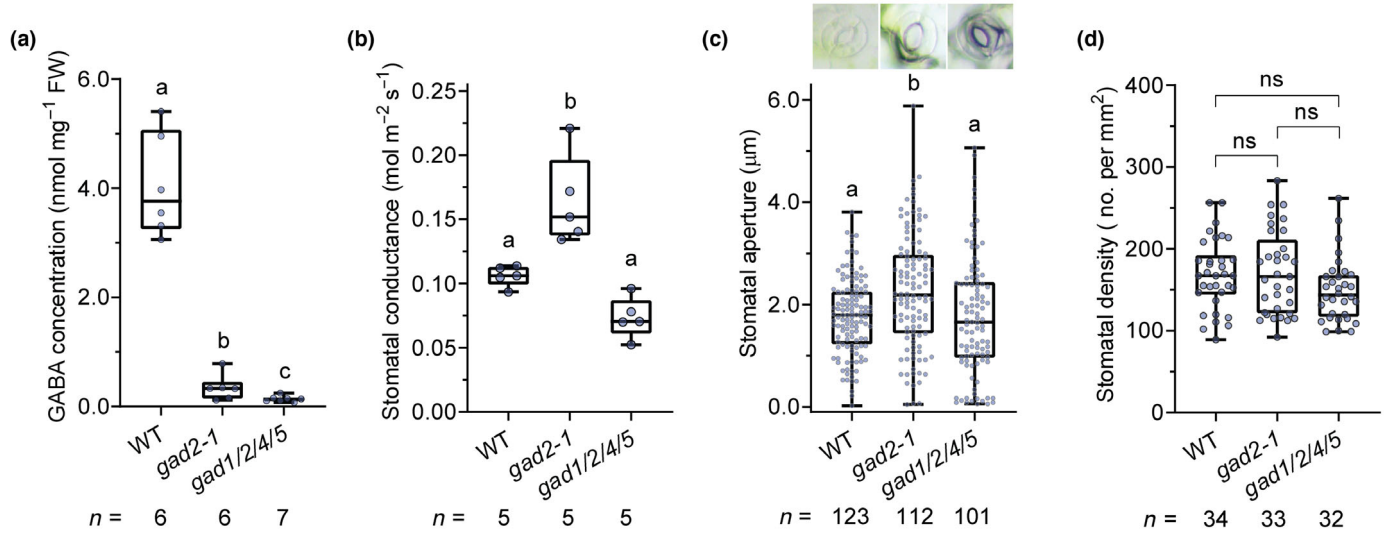

Fig. 1 Stomatal phenotypes of the *gad2-1* mutant are lost following ablation of *GAD1*, *GAD4*, and *GAD5*. (a–d) GABA concentration (a), stomatal conductance (b), aperture width (c) and density (d) of 5–6 wk-old Arabidopsis wild-type (WT) Col-0, *gad2-1*, and *gad1/2/4/5* plants. (a) GABA concentration in the leaves of 5–6 wk-old Arabidopsis WT, *gad2-1*, and *gad1/2/4/5* mutant plants, data extracted from Supporting Information Fig. S1(b); FW, fresh weight. (b) Stomatal conductance was determined by AP4 Porometer. (c) Epidermal strips were incubated in stomatal pore measurement buffer for 2 h under light (200 μmol m^{-2} s^{-1}) before stomatal aperture measurement. (d) Stomatal densities on abaxial leaf surfaces were determined on WT, *gad2-1*, and *gad1/2/4/5* plants. Replicate number as indicated within graph (*n*). Box plots indicate first quartile, median, and third quartile values; whiskers show minimum and maximum values. Different letters indicate significant differences following statistical analysis by multiple *t*-test ($P < 0.05$, a) or one-way ANOVA with Tukey's *post hoc* test ($P < 0.05$, b; $P < 0.01$, c, d); ns, not significant.

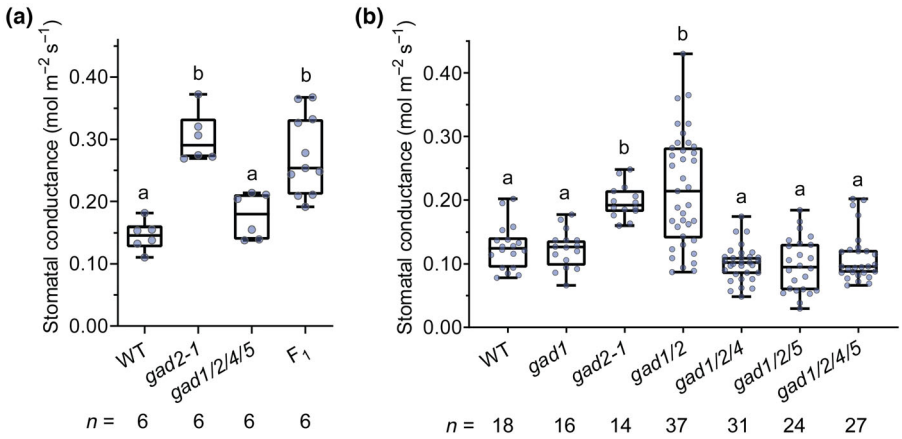

Fig. 2 Loss of *GAD4* or *GAD5* compromises the *gad2-1* stomatal conductance. (a) Stomatal conductance of 5–6 wk-old Arabidopsis wild-type (WT), *gad2-1*, *gad1/2/4/5* mutants and F_1 (F_1 *gad2-1* × *gad1/2/4/5* generation crosses, equivalent to *gad2-1* single mutant) as determined by AP4 Porometer. (b) Stomatal conductance of 5–6 wk-old Arabidopsis WT, *gad1*, *gad2-1*, *gad1/2*, *gad1/2/4*, *gad1/2/5* and *gad1/2/4/5*; *gad1/2*, *gad1/2/4* and *gad1/2/5* were segregated from F_1 *gad2-1* × *gad1/2/4/5* as indicated in (a). Replicate number as indicated within graph (*n*). Box plots indicate first quartile, median, and third quartile values; whiskers show minimum and maximum values. Different letters indicate significant differences at $P < 0.05$, following statistical analysis by one-way ANOVA with Tukey's *post hoc* test.

as ROS production (Kong *et al.*, 2016; Yoshida *et al.*, 2016; Fichman *et al.*, 2021). Glu has also been proposed to trigger apoplastic calcium influx into guard cells and close stomata (Yoshida *et al.*, 2016). We detected greater Glu content in leaves of *gad2-1* and the higher order *gad* mutants than in WT, with a significantly higher Glu content in *gad1/2/4/5* than in *gad2-1* leaves (Fig. S1c). Therefore, we compared the stomatal sensitivity of WT, *gad2-1*, and *gad1/2/4/5* guard cells to externally supplied Glu. Consistent with the previous research, 1 mM Glu closed the stomata of Arabidopsis WT plants under constant light in the presence of 50 μM Ca^{2+}, whilst 1 mM GABA had no effect (Fig. S2a,d; Yoshida *et al.*, 2016; Xu *et al.*, 2021a). Glu also stimulated stomatal closure in *gad2-1* (Fig. S2b,e) but not in *gad1/2/4/5* leaves (Fig. S2c,f). The additional supplement of the Ca^{2+} channel blocker lanthanum chloride ($LaCl_3$) (Harada & Shimazaki, 2009) antagonized Glu-induced stomatal closure in WT and *gad2-1* but had no effect on *gad1/2/4/5* stomata (Fig. S2a–c). In the presence of 50 μM Ca^{2+} supplementation with EGTA, a calcium chelator commonly used to reduce apoplast-derived cytosolic Ca^{2+} increases, not only antagonized the Glu effect in *gad2-1* and WT

stomata but also increased the aperture of all genotypes by itself, including *gad1/2/4/5* (Fig. S2d–f). The effect of lowering of apoplastic Ca^{2+} on different genotypes was further examined by removing Ca^{2+} from the stomatal measurement buffer and lowering the EGTA supplement from 1 mM to 200 μM. In these conditions, no impact on the stomatal apertures of WT or *gad2-1* leaves was observed, but *gad1/2/4/5* stomatal aperture significantly increased, similar to that of *gad2-1* (Fig. 3a), suggesting that impaired Ca^{2+} homeostasis in *gad1/2/4/5* guard cells may contribute to its stomatal phenotype. To directly test this, we used a Ca^{2+} and pH dual sensor (CapHensor) to investigate guard-cell cytosolic Ca^{2+} and proton (H^+) (Li *et al.*, 2021) and found in replicated experiments that a higher Ca^{2+} concentration ratio was detected in the guard cells of *gad1/2/4/5* compared with WT and *gad2-1* mutants, whilst the H^+ concentration ratio was unchanged (Fig. 4). These data suggest that the resting cytosolic Ca^{2+} concentration, but not pH, is affected by the severe impairment in GABA synthesis found in *gad1/2/4/5* compared with the lesser impaired *gad2-1* (Fig. 1). Furthermore, to test whether impaired GABA synthesis was linked to ROS or NO, as suggested in Bor & Turkan (2019), we measured ROS and NO production in the guard cells using H_2DCF-DA and DAF-2DA, respectively. We found that only ROS accumulation, not that of NO, was elevated in *gad1/2/4/5* guard cells compared to those from WT and *gad2-1* leaves and that ROS accumulation decreased to that of the WT and *gad2-1* by limiting apoplastic Ca^{2+} with EGTA treatment (Figs 3b, 5a, S3). The greater variation in Ca^{2+} concentration in *gad1/2/4/5* guard cells mirrors the greater variation also seen in ROS accumulation (Figs 4, 5).

To more directly determine whether altered ROS homeostasis contributes to the differential stomatal phenotype of *gad2-1* and *gad1/2/4/5*, we applied various ROS inhibitors to epidermal strips

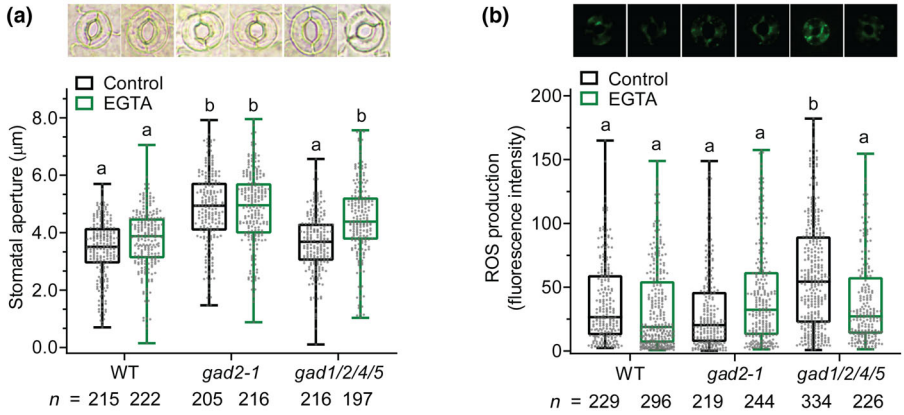

Fig. 3 Reactive oxygen species (ROS) accumulation is greater and stomatal conductance lower in *gad1/2/4/5* compared with *gad2-1*, but can be complemented by reducing apoplastic Ca^{2+}. (a, b) Stomatal aperture (a) and guard-cell ROS production (b) of Arabidopsis wild-type (WT), *gad2-1* and *gad1/2/4/5* mutant plants. Epidermal strips were pre-incubated in stomatal pore measurement buffer for 1 h under light (200 μmol m^{-2} s^{-1}) and transferred to buffers with or without 200 μM EGTA supplementation for 2 h to reduce apoplastic Ca^{2+} before stomatal aperture (a) or guard-cell ROS (b) measurement, replicate number as indicated within graph (*n*). Box plots indicate first quartile, median, and third quartile values; whiskers show minimum and maximum values. Different letters indicate significant differences at $P < 0.01$, following statistical analysis by two-way ANOVA. Assay buffer had no added calcium.

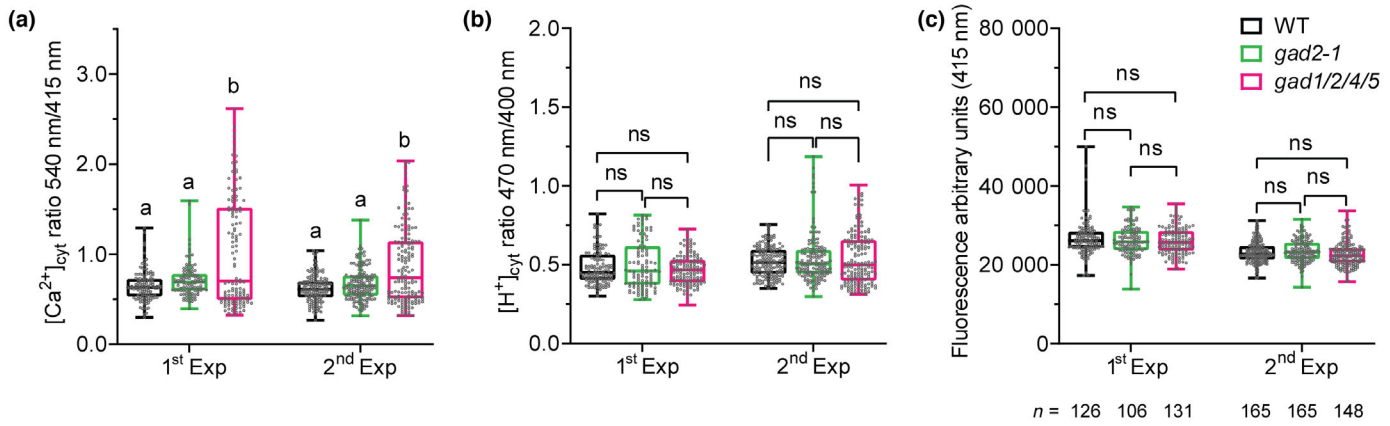

Fig. 4 Higher cytosolic Ca^{2+} concentration ratio is detected in the guard cells of the *gad1/2/4/5* mutant. (a, c) Cytosolic Ca^{2+} ($[Ca^{2+}]_{cyt}$) (a) and H^+ ($[H^+]_{cyt}$) (b) ratio of ROI were calculated based on R-GECO1$_{540\ nm}$/PRpHluorin$_{415\ nm}$ and PRpHluorin$_{470\ nm}$/PRpHluorin$_{400\ nm}$, as described in Li *et al*. (2021); and the arbitrary units of PRpHluorin fluorescence excited at 415 nm (known as the isosbestic point; Li *et al*., 2021) was plotted as an internal control to determine CapHensor protein expression levels within Arabidopsis wild-type (WT) and *gad* mutant plants (c). Replicate number as indicated within graph (*n*). Box plots indicate first quartile, median, and third quartile values; whiskers show minimum and maximum values. Different letters indicate significant differences at $P < 0.01$, following statistical analysis by multiple *t*-test using a nonparametric test; ns, not significant.

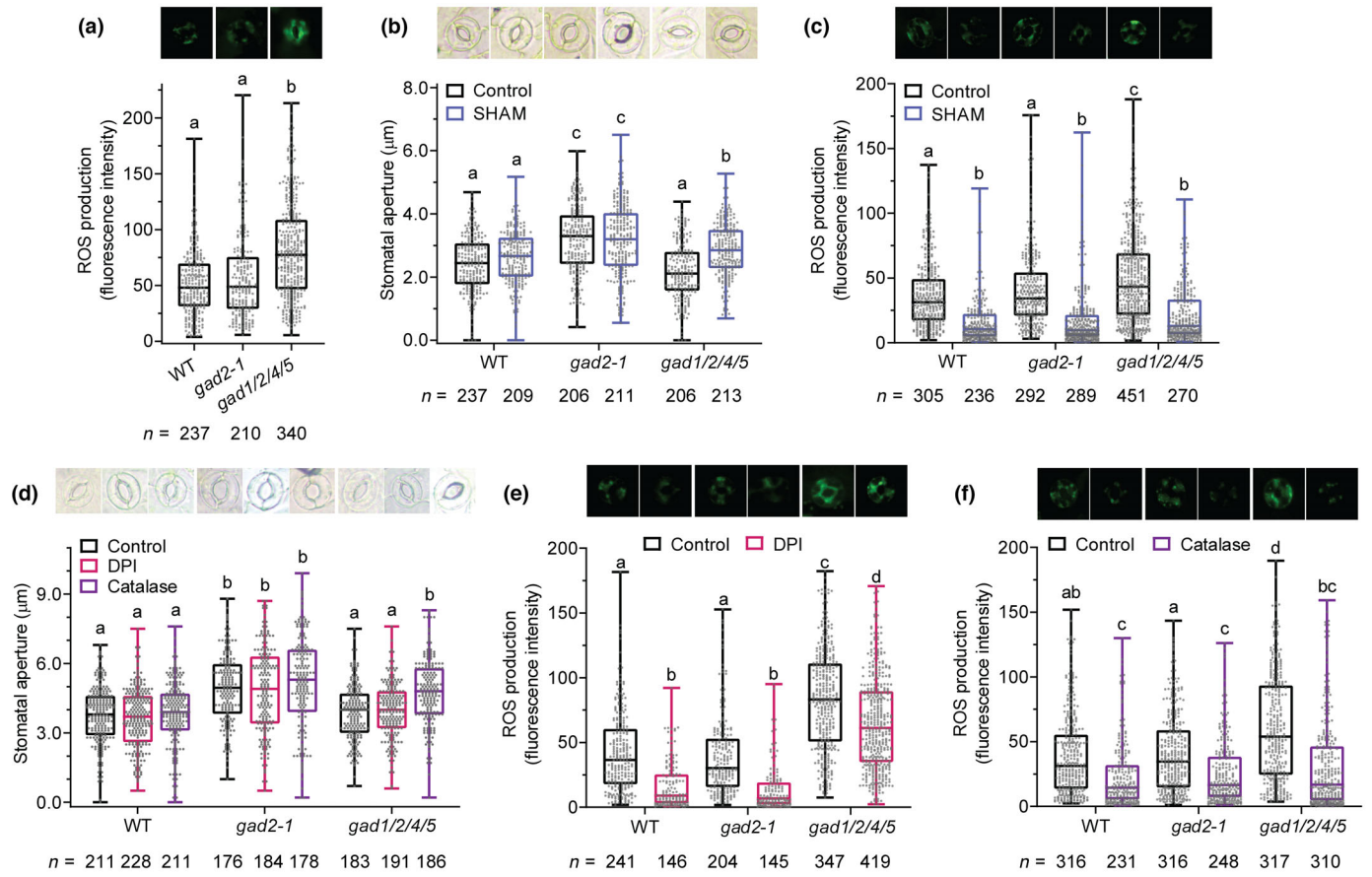

Fig. 5 Greater reactive oxygen species (ROS) production in guard cells in the *gad1/2/4/5* mutant reduces its stomatal apertures to that of wild-type. (a–f) Guard-cell ROS production and stomatal aperture of Arabidopsis wild-type (WT), *gad2-1* and *gad1/2/4/5* mutant plants. Epidermal strips were pre-incubated in stomatal pore measurement buffer for 1 h under light (200 μmol m^{-2} s^{-1}) and transferred to the same buffer (a) or buffers supplemented with 2 mM SHAM (b, c), 20 μM DPI (d, e) or 100 U ml^{-1} catalase (d, f) for 2 h before guard-cell ROS (a, c, e, f) or stomatal aperture (b, d) measurement. Replicate number as indicated within graph (*n*). Box plots indicate first quartile, median, and third quartile values; whiskers show minimum and maximum values. Different letters indicate significant differences at $P < 0.01$, following statistical analysis by one-way ANOVA with Tukey's *post hoc* test (a) or two-way ANOVA (b–f). The same leaf areas were measured for all samples, the smaller replicates for stomata with lower ROS are a consequence of detection limits (i.e. stomata with zero signal were not counted).

and found that the stomatal aperture of *gad1/2/4/5* was increased by a class III plant peroxidase inhibitor SHAM and catalase (that degrades H_2O_2), both of which reduce guard-cell ROS production (Fig. 5b–d,f). Intriguingly, the apoplastic NADPH oxidase inhibitor DPI, which has been previously implicated in Glu- and ROS-induced stomatal closure (Kong *et al.*, 2016), did not reduce guard-cell ROS of *gad1/2/4/5* to that of the WT, nor reduce the stomatal aperture (Fig. 5d–f). No difference was detected in loading of the ROS indicators between genotypes (Fig. S4), so collectively these data suggest a biological link between GABA and ROS accumulation. Previously, links have been made between peroxidase activity and GABA accumulation (Krush & Rastegar, 2023), which may indicate an imbalance in the ROS homeostasis when GAD activity is abolished. Furthermore, explicit links between chloroplastic H_2O_2 stimulating GABA production through GAD have been made (Maruta *et al.*, 2013). As such, it is possible that GABA plays a major role in quenching chloroplast-generated cytoplasmic ROS, rather than that of apoplastic-generated ROS through NADPH oxidase.

The ROS inhibitors we used reduced basal ROS production in the guard cells of WT plants and *gad2-1* but did not alter stomatal aperture (Fig. 5b–f), suggesting that a decrease in basal guard-cell ROS production does not directly affect stomatal pore size, consistent with the previous research (Li *et al.*, 2016, 2018). Both *gad2* mutants and the *gad1/2* mutant had similar guard-cell ROS production to WT plants, whilst higher order mutants (*gad1/2/4/5*, *gad1/2/4*, and *gad1/2/5*) all produced greater ROS in their guard cells (Fig. S5a,b). This result likely explains why *gad1/2/4*, *gad1/4/5*, and *gad1/2/4/5* have WT-like stomatal phenotypes, unlike *gad2-1* and *gad1/2*, although all lines have depleted GABA in leaves (Fig. S1).

To further test the impact of GABA on ROS and stomatal conductance, we transformed the *gad1/2/4/5* mutant with an active form of *GAD2* (*GAD2Δ*) driven by the guard-cell-specific promoter *GC1* (*GC1::GAD2Δ*), which we previously used to increase GABA in *gad2* lines in Xu *et al.* (2021a). We recovered three independent *gad1/2/4/5*/*GC1::GAD2Δ* lines, all of which complemented ROS accumulation back to WT levels compared

with the significantly greater values seen in *gad1/2/4/5* (Fig. 6a). Intriguingly, two ROS complemented lines had an increased stomatal conductance (*gad1/2/4/5/GC1::GAD2Δ* #4 and #5, or lines #4 and #5), whereas the other *gad1/2/4/5/GC1::GAD2Δ* #2 (line #2) presented a WT-like stomatal conductance (Fig. 6b). As we have shown that *gad1/2/4/5* has significantly greater ROS accumulation than all other lines tested (e.g. Fig. 6a) and that quenching ROS in *gad1/2/4/5* increases stomatal aperture (Figs 3, 5), we investigated the relationship between GABA and stomatal conductance in our material with comparable ROS (Fig. 6c) (i.e. the complementation lines and WT, excluding *gad1/2/4/5* which accumulates significantly greater ROS (Fig. 6a,c)). When examining these lines with equal ROS, we found stomatal conductance to be significantly negatively correlated with GABA concentration ($P < 0.001$; Fig. 6c). We interpret this result as a clear demonstration that GABA can impact stomatal conductance in two ways: (1) When GABA is low but sufficient to quench ROS (e.g. *gad1/2/4/5/GC1::GAD2Δ* #4 and #5) (Figs 1, 6a), yet insufficient to constrain stomatal opening, this phenocopies the large stomatal aperture of *gad2-1* (Figs 1, 6c; Xu *et al.*, 2021a) and (2) a further rise in GABA accumulation, as observed in *gad1/2/4/5/GC1::GAD2Δ* #2, constrains stomatal opening leading to WT-like stomatal performance (Fig. 6), as is seen in WT and also *gad2-1/GC1::GAD2Δ* (Xu *et al.*, 2021a).

The GABA shunt is the major pathway for GABA metabolism in plants, which bypasses ROS-sensitive steps of TCA cycle and comprises three key enzymes – GAD, GABA-T, and SSADH (Gilliham & Tyerman, 2016). Under stress, the *ssadh* and *gad1/2* T-DNA knockout mutants have been associated with higher ROS production, whereas *gaba-t/pop2* (with greater GABA accumulation) has lower ROS production (Bouché *et al.*, 2003; Su *et al.*, 2019; Wu *et al.*, 2021); collectively, this suggests the GABA shunt mediates ROS homeostasis under stress. However, none of these studies have found that GABA metabolism alters basal ROS production under nonstressed conditions. Here, we used the *gad1/2/4/5* mutant and its complementation lines to study the impact of low tissue GABA on guard cell function. Much to our surprise, whilst *gad1/2/4/5* had a lower leaf GABA content than *gad2-1* and *gad2-2*, it did not share the two *gad2* mutant's greater stomatal apertures and conductance; in fact, we found that it possessed WT-like stomatal apertures and conductance. On initial observation, despite two independent alleles of *gad2* sharing the same stomatal phenotype and their phenotypic complementation by *GAD2*, *gad1/2/4/5* not sharing the same stomatal phenotype as *gad2* could be seen to call the role of GABA as a regulator of guard cell opening into question (Xu *et al.*, 2021a). On closer examination, we have been able to determine – through multiple lines of evidence – that the *gad1/2/4/5* quadruple knockout impairs guard-cell ROS homeostasis, which compromises the higher stomatal conductance and aperture caused by GABA deficiency observed in the *gad2* single mutants (Figs 1, 5a; Xu *et al.*, 2021a). By reducing ROS in the *gad1/2/4/5* background, we can clearly restore the negative relationship between GABA accumulation and stomatal conductance (Fig. 6c). Despite the very low expression of *GAD4* and *GAD5* in leaves under standard conditions, they appear to have a major impact on stomatal phenotype when *GAD2* is also ablated in guard cells.

The high ROS accumulation phenotype of *gad1/2/4/5* guard cells under control conditions and the greater stress induced ROS within *gad1/2* roots suggests the impact of GADs are differential but additive, and together with the lesser ROS in *pop2/gaba-t* lines (high GABA) (Wu *et al.*, 2021), this is consistent with GABA and

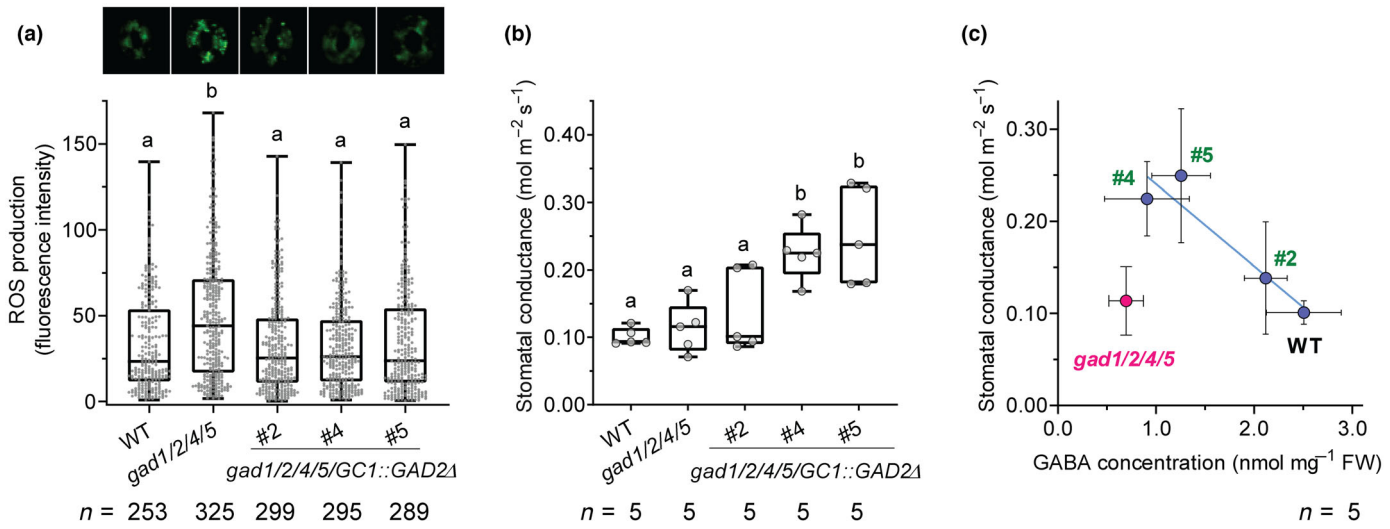

Fig. 6 Complementation of *GAD2Δ* reduces guard-cell reactive oxygen species (ROS) production and increases either GABA accumulation in leaves or stomatal conductance of *gad1/2/4/5* mutant. (a, b) Guard-cell ROS production (a) and stomatal conductance (b) of Arabidopsis wild-type (WT), *gad1/2/4/5* mutants and complementation plants. Guard-cell *GAD2Δ* complementation (*GC1::GAD2Δ*) in *gad1/2/4/5* restored guard-cell ROS production of *gad1/2/4/5/GC1::GAD2Δ* #2, #4 and #5 lines (lines #2, #4 and #5) to WT levels (a), and gradually increased the stomatal conductance of lines #2, #4 and #5 (b). (c) Leaf GABA concentration quantified by GABase vs stomatal conductance in Arabidopsis WT, *gad1/2/4/5* and complementation plants (lines #2, #4 and #5), a linear regression was plotted for WT, lines #2, #4 and #5 with an $R^2 = 0.6$ and $P = 0.000145$; FW, fresh weight. Red circle indicates high ROS and blue circle indicates normal ROS (see a). Replicate number as indicated within graph (*n*). Data represent mean ± SD (c); or box plots indicate first quartile, median, and third quartile values; whiskers show minimum and maximum values (a, b). Different letters indicate significant differences at $P < 0.01$ with high number of replicates (a) or $P < 0.05$ with five replicates (b), following statistical analysis by one-way ANOVA with Tukey's *post hoc* test.

GADs being a key physiological mechanism for the modulation of ROS as a signalling agent under both standard and stressed conditions. There is evidence to suggest that GABA concentration (and some *GAD* expression) is diel regulated, reaching a maximum in early morning after exposure to light, then decreasing until the next light cycle, except under stress when GABA is constitutively high (Espinoza *et al.*, 2010). This suggests that GABA may have more influence over ROS at these times, quenching ROS when stomata are opening and/or most open under standard conditions and having a lesser role when stomata are primed for closure. Moving forward, it would now be important to build better understanding of how *GAD* expression and GABA concentration is regulated and coordinated at the single-cell level to further explore the roles of the various *GAD* paralogs in whole plant function with respect to GABA's role in quenching ROS.

In addition to our study highlighting – again – the importance of single-cell processes and how they may be masked by examination of whole leaf phenotypes, it also raises a new question of how GABA, Glu, and ROS interact to maintain autonomous Ca^{2+} homeostasis in the guard cells. We found that chelation of apoplastic Ca^{2+} reduced both guard-cell ROS production and the enlarged stomatal aperture of *gad1/2/4/5* leaves (Fig. 3) and that *gad1/2/4/5* stomata are insensitive to Glu (Fig. S2). These data suggest that the increased ROS production in *gad1/2/4/5* guard cells may well be linked to impaired Ca^{2+} homeostasis, which may be triggered by higher Glu content in *gad1/2/4/5* leaves relative to *gad2-1* or WT leaves; however, the *gad1/2* mutant also has higher Glu and lower ROS, so further work needs to be conducted to explore the link with Glu (Fig. S1). As both Ca^{2+} and ROS can act both up and downstream of each other (Murata *et al.*, 2015; Medeiros *et al.*, 2020), we cannot confirm the exact order of events. Furthermore, as there are 20 GLRs, and as we already working in a quadruple mutant background, we have not been able to confirm, at this point in time, if GLRs are responsible for *gad* induced changes in Ca^{2+} and ROS. Further research will now be required to explore how plants balance GABA and Glu signalling via the GABA shunt to impact plant phenotypes as foreshadowed in Xu *et al.* (2021b), and examine the exact mechanism by which GABA controls ROS accumulation.

Our work has shed new light on the complexity of GABA signalling in plants and its role in modulating plant gas exchange. Previously, it was shown that GABA affects ABA, coronatine, and light- and dark-induced stomatal opening and closure (Xu *et al.*, 2021a). γ-Aminobutyric acid is also known to impact the activity of Aluminium-activated Malate Transporters and is suggested to have other targets such as potassium channels or proton pumps (Ramesh *et al.*, 2015, 2017; Xu *et al.*, 2021b). Here, we show that GABA metabolism impacts ROS production and Glu accumulation in plants and adds further points of interaction for GABA as a signalling molecule.

Acknowledgements

We thank Larissa Chirkova and Mamoru Okamoto for performing UPLC measurements. We acknowledge the support of the Australian Research Council (DP210102828) awarded to MG, RH and JK for funding this work. Open access publishing facilitated by The University of Adelaide, as part of the Wiley - The University of Adelaide agreement via the Council of Australian University Librarians.

Competing interests

None declared.

Author contributions

BX, SZ, JK, RH, KRK and MG supervised the research. BX performed stomatal aperture, Ca^{2+}-pH imaging and ROS measurements. XF performed stomatal conductance measurements, segregated and genotyped the *gad* mutants, prepared samples for GABA and Glu measurement, and constructed complemented plants. AP performed the stomatal density measurements and verified experimental data independently. BX and XF contributed equally to this work.

ORCID

Xueying Feng https://orcid.org/0000-0002-9573-6082
Matthew Gilliham https://orcid.org/0000-0003-0666-3078
Rainer Hedrich https://orcid.org/0000-0003-3224-1362
Kai R. Konrad https://orcid.org/0000-0003-4626-5429
Johannes Kromdijk https://orcid.org/0000-0003-4423-4100
Adriane Piechatzek https://orcid.org/0000-0002-7958-5771
Bo Xu https://orcid.org/0000-0002-7583-2384
Shuqun Zhang https://orcid.org/0000-0003-2959-6461

Data availability

The data supporting the findings of this study are available in the Supporting Information of this article.

References

Agurla S, Gayatri G, Raghavendra AS. 2016. Nitric oxide (NO) measurements in stomatal guard cells. In: Gupta K, ed. *Plant nitric oxide: methods and protocols*. New York, NY, USA: Humana Press, 49–56.

Balfagón D, Gómez-Cadenas A, Rambla JL, Granell A, de Ollas C, Bassham DC, Mittler R, Zandalinas SI. 2022. γ-Aminobutyric acid plays a key role in plant acclimation to a combination of high light and heat stress. *Plant Physiology* **188**: 2026–2038.

Bor M, Turkan I. 2019. Is there a room for GABA in ROS and RNS signalling? *Environmental and Experimental Botany* **161**: 67–73.

Bouché N, Fait A, Zik M, Fromm H. 2004. The root-specific glutamate decarboxylase (GAD1) is essential for sustaining GABA levels in Arabidopsis. *Plant Molecular Biology* **55**: 315–325.

Bouché N, Lacombe B, Fromm H. 2003. GABA signaling: a conserved and ubiquitous mechanism. *Trends in Cell Biology* **13**: 607–610.

Bown AW, Shelp BJ. 2016. Plant GABA: not just a metabolite. *Trends in Plant Science* **21**: 811–813.

Deng X, Xu X, Liu Y, Zhang Y, Yang L, Zhang S, Xu J. 2020. Induction of γ-aminobutyric acid plays a positive role to Arabidopsis resistance against *Pseudomonas syringae*. *Journal of Integrative Plant Biology* **62**: 1797–1812.

Espinoza C, Degenkolbe T, Caldana C, Zuther E, Leisse A, Willmitzer L, Hincha DK, Hannah MA. 2010. Interaction with diurnal and circadian regulation results

in dynamic metabolic and transcriptional changes during cold acclimation in Arabidopsis. *PLoS ONE* **5**: e14101.

Fait A, Yellin A, Fromm H. 2005. GABA shunt deficiencies and accumulation of reactive oxygen intermediates: insight from Arabidopsis mutants. *FEBS Letters* **579**: 415–420.

Fichman Y, Myers RJ, Grant DG, Mittler R. 2021. Plasmodesmata-localized proteins and ROS orchestrate light-induced rapid systemic signaling in Arabidopsis. *Science Signaling* **14**: 1–12.

Fromm H. 2020. GABA signaling in plants: targeting the missing pieces of the puzzle. *Journal of Experimental Botany* **71**: 6238–6245.

Gilliham M, Tyerman SD. 2016. Linking metabolism to membrane signaling: the GABA-malate connection. *Trends in Plant Science* **21**: 295–301.

Harada A, Shimazaki K. 2009. Measurement of changes in cytosolic Ca^{2+} in Arabidopsis guard cells and mesophyll cells in response to blue light. *Plant and Cell Physiology* **50**: 360–373.

Kong D, Hu H-C, Okuma E, Lee Y, Lee HS, Munemasa S, Cho D, Ju C, Pedoeim L, Rodriguez B. 2016. L-Met activates Arabidopsis GLR Ca^{2+} channels upstream of ROS production and regulates stomatal movement. *Cell Reports* **17**: 2553–2561.

Krush GH, Rastegar S. 2023. γ-Aminobutyric acid (GABA) inhibits the enzymatic browning of cut *Narcissus tazetta* cv.'Shahla-e-Shiraz' flowers during vase life. *Journal of Plant Growth Regulation* **42**: 2602–2612.

Li K, Prada J, Damineli DS, Liese A, Romeis T, Dandekar T, Feijó JA, Hedrich R, Konrad KR. 2021. An optimized genetically encoded dual reporter for simultaneous ratio imaging of Ca^{2+} and H^+ reveals new insights into ion signaling in plants. *New Phytologist* **230**: 2292–2310.

Li Y, Xu S, Gao J, Pan S, Wang G. 2016. Glucose- and mannose-induced stomatal closure is mediated by ROS production, Ca^{2+} and water channel in *Vicia faba*. *Physiologia Plantarum* **156**: 252–261.

Li Y, Xu S, Wang Z, He L, Xu K, Wang G. 2018. Glucose triggers stomatal closure mediated by basal signaling through HXK1 and PYR/RCAR receptors in Arabidopsis. *Journal of Experimental Botany* **69**: 1471–1484.

Maruta T, Ojiri M, Noshi M, Tamoi M, Ishikawa T, Shigeoka S. 2013. Activation of γ-aminobutyrate production by chloroplastic H_2O_2 is associated with the oxidative stress response. *Bioscience, Biotechnology, and Biochemistry* **77**: 422–425.

Medeiros DB, Barros JA, Fernie AR, Araújo WL. 2020. Eating away at ROS to regulate stomatal opening. *Trends in Plant Science* **25**: 220–223.

Mekonnen DW. 2017. Oversensitivity of Arabidopsis *gad1/2* mutant to NaCl treatment reveals the importance of GABA in salt stress responses. *African Journal of Plant Science* **11**: 252–263.

Mekonnen DW, Flügge U-I, Ludewig F. 2016. Gamma-aminobutyric acid depletion affects stomata closure and drought tolerance of *Arabidopsis thaliana*. *Plant Science* **245**: 25–34.

Murata Y, Mori IC, Munemasa S. 2015. Diverse stomatal signaling and the signal integration mechanism. *Annual Review of Plant Biology* **66**: 369–392.

Palanivelu R, Brass L, Edlund AF, Preuss D. 2003. Pollen tube growth and guidance is regulated by POP2, an Arabidopsis gene that controls GABA levels. *Cell* **114**: 47–59.

Ramesh SA, Kamran M, Sullivan W, Chirkova L, Okamoto M, Degryse F, McLauchlin M, Gilliham M, Tyerman SD. 2018. Aluminium-activated malate transporters can facilitate GABA transport. *Plant Cell* **30**: 1147–1164.

Ramesh SA, Tyerman SD, Gilliham M, Xu B. 2017. γ-Aminobutyric acid (GABA) signalling in plants. *Cellular and Molecular Life Sciences* **74**: 1577–1603.

Ramesh SA, Tyerman SD, Xu B, Bose J, Kaur S, Conn V, Domingos P, Ullah S, Wege S, Shabala S *et al.* 2015. GABA signalling modulates plant growth by directly regulating the activity of plant-specific anion transporters. *Nature Communications* **6**: 1–9.

Schneider CA, Rasband WS, Eliceiri KW. 2012. NIH Image to ImageJ: 25 years of image analysis. *Nature Methods* **9**: 671–675.

Scholz SS, Reichelt M, Mekonnen DW, Ludewig F, Mithöfer A. 2015. Insect herbivory-elicited GABA accumulation in plants is a wound-induced, direct, systemic, and jasmonate-independent defense response. *Frontiers in Plant Science* **6**: 1–11.

Shi SQ, Shi Z, Jiang ZP, Qi LW, Sun XM, Li CX, Liu JF, Xiao WF, Zhang SG. 2010. Effects of exogenous GABA on gene expression of *Caragana intermedia* roots under NaCl stress: regulatory roles for H_2O_2 and ethylene production. *Plant, Cell & Environment* **33**: 149–162.

Su N, Wu Q, Chen J, Shabala L, Mithöfer A, Wang H, Qu M, Yu M, Cui J, Shabala S. 2019. GABA operates upstream of H^+-ATPase and improves salinity tolerance in Arabidopsis by enabling cytosolic K^+ retention and Na^+ exclusion. *Journal of Experimental Botany* **70**: 6349–6361.

Wu Q, Su N, Huang X, Cui J, Shabala L, Zhou M, Yu M, Shabala S. 2021. Hypoxia-induced increase in GABA content is essential for restoration of membrane potential and preventing ROS-induced disturbance to ion homeostasis. *Plant Communications* **2**: 1–12.

Xu B, Long Y, Feng X, Zhu X, Sai N, Chirkova L, Betts A, Herrmann J, Edwards JE, Okamoto M *et al.* 2021a. GABA signalling modulates stomatal opening to enhance plant water use efficiency and drought resilience. *Nature Communications* **12**: 1–13.

Xu B, Sai N, Gilliham M. 2021b. The emerging role of GABA as a transport regulator and physiological signal. *Plant Physiology* **187**: 2005–2016.

Yoshida R, Mori IC, Kamizono N, Shichiri Y, Shimatani T, Miyata F, Honda K, Iwai S. 2016. Glutamate functions in stomatal closure in Arabidopsis and fava bean. *Journal of Plant Research* **129**: 39–49.

Zhu M, Jeon BW, Geng S, Yu Y, Balmant K, Chen S, Assmann SM. 2016. Preparation of epidermal peels and guard cell protoplasts for cellular, electrophysiological, and -omics assays of guard cell function. In: Botella JR, Botella MA, eds. *Plant signal transduction*. New York, NY, USA: Humana Press, 89–121.

Supporting Information

Additional Supporting Information may be found online in the Supporting Information section at the end of the article.

Fig. S1 Loss of *GAD4* or *GAD5* compromises the *gad2-1* stomatal pore aperture.

Fig. S2 Glutamate closes stomata of wild-type and *gad2-1*, but not *gad1/2/4/5* in presence of 50 μM $CaCl_2$.

Fig. S3 Guard-cell NO production is similar between wild-type and *gad* mutants.

Fig. S4 Guard-cell ROS production, excited by mercury lamp for *c.* 20 s, is similar between wild-type and *gad* mutants, suggesting the guard cells of different genotypes plants all contains similar levels of H_2DCF-DA before imaging.

Fig. S5 Loss of *GAD4* or *GAD5* increases guard-cell ROS production in *gad1/2* mutant.

Table S1 Primer sets used to identify T-DNA insertion in Arabidopsis *gad* mutants.

Please note: Wiley is not responsible for the content or functionality of any Supporting Information supplied by the authors. Any queries (other than missing material) should be directed to the *New Phytologist* Central Office.